CRYSTAL GROWTH & DESIGN

Article

pubs.acs.org/crystal

# Structures, Luminescence, and Magnetic Properties of Several Three-Dimensional Lanthanide–Organic Frameworks Comprising 4-Carboxyphenoxy Acetic Acid

Peng-fei Shi, Zhi Chen, Gang Xiong, Bo Shen, Jing-Zhe Sun, Peng Cheng,* and Bin Zhao*

Department of Chemistry, Key Laboratory of Advanced Energy Material Chemistry, MOE, and TKL of Metal and Molecule Based Material Chemistry, Nankai University, Tianjin 300071, China

Supporting Information

**ABSTRACT:** Ten new 3D lanthanide-based compounds, $\{[Ln_4(CPOA)_6(H_2O)_4]\cdot H_2O\}_n$ (Ln = Eu (**1**), Gd (**2**), Tb (**3**), Dy (**4**), Ho (**5**)) and $[Ln(CPOA)(C_2O_4)_{0.5}(H_2O)]_n$ (Ln = Eu (**1a**), Gd (**2a**), Tb (**3a**), Dy (**4a**), Ho (**5a**)) ($CPOA^{2-}$ = 4-carbomethoxybenzoate), have been synthesized by a hydrothermal method under different temperatures. The compounds **1**–**5** were obtained at 140 °C. When the temperature went up to 180 °C, the ligands partly decomposed to $C_2O_4^{2-}$, then came into being compounds **1a**–**5a**. The two series of compounds displayed the differences not only in structure but also in thermal stability and luminescent and magnetic properties. Compounds **1**–**5** crystallize in the triclinic system, space group $P\bar{1}$, whereas compounds **1a**–**5a** belong to the monoclinic system with space group $P2_1/c$. Thermal analyses were carried out on **1**–**5** and **1a**–**3a**. Solid luminescence studies of compounds **1** and **1a**, **3** and **3a**, and **4** and **4a** show the characteristic bands of $Eu^{3+}$, $Tb^{3+}$, and $Dy^{3+}$, respectively. Magnetic properties were investigated on **2**–**4** and **2a**–**4a**. The out-of-phase signals ($\chi_M''$) of **4** exhibit a strong frequency dependence, suggesting the existence of slow magnetic relaxation behavior in **4**.

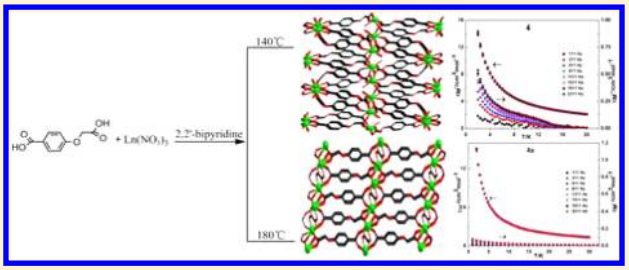


## INTRODUCTION

The fabrication of lanthanide-based compounds has been attractive and has a bright future in constructing multifunctional materials due to their structural diversities, and extensive applications in many fields.[1−7] Especially in magnetic properties, large spin ground state and high spin–orbit coupling of lanthanide ions are apt to bring large magnetic anisotropy, which is critical for single-molecule magnets (SMMs) and single-chain magnets (SCMs). Thus, compounds based on lanthanide ions may have particular advantages in constructing novel magnetic materials.[8] For example, SMMs and SCMs based on Dy(III) have been well-reported.[9] However, the report of the slow magnetic relaxation behavior existing in 2D or 3D lanthanide–organic frameworks (LOFs) is relatively rare.[10] Therefore, it is interesting and worthy of exploiting the magnetic properties in multidimensional compounds. On the other hand, as a result of the particular f–f transition of lanthanide ions, the luminescent properties of compounds containing lanthanide ions usually feature narrow emission peaks and little influence of the ambient environment. Consequently, these compounds may become unique luminescent materials.[11]

As known, the selection of ligands plays a key role in assembling coordination polymers, because the slight change of the ligands, such as symmetry, flexibility, and the number of coordinated atoms, may result in dramatic differences in structures and properties. Accordingly, the reported LOFs, organic aromatic multicarboxylate ligands, are frequently chosen to fabricate various topological frameworks as for their rich coordination modes and flexible configurations.[12] We selected the 4-carboxyphenoxy acetic acid ($H_2CPOA$) as the ligand to design and synthesize 3D LOFs with the following reasons: (1) lack of symmetry in the positioning of carboxylate groups in the ligand, −COOH and $-OCH_2COOH$, which benefit for structural tunability; (2) owning a rigid benzene ring and a flexible $-OCH_2COOH$ spacer, which make $H_2CPOA$ possess variable configurations; (3) the reported compounds containing this ligand mostly focused on transitional-metal compounds.[13]

As a continuation of our previous work,[14] herein we successfully synthesized 10 LOFs with the $H_2CPOA$ ligand by a hydrothermal method under different reaction temperatures, $\{[Ln_4(CPOA)_6(H_2O)_4]\cdot H_2O\}_n$ (Ln = Eu (**1**), Gd (**2**), Tb (**3**), Dy (**4**), Ho (**5**)) and $[Ln(CPOA)(C_2O_4)_{0.5}(H_2O)]_n$ (Ln = Eu (**1a**), Gd (**2a**), Tb (**3a**), Dy (**4a**), Ho (**5a**)), among which, the $C_2O_4^{2-}$ may arise from the decomposition of the $H_2CPOA$ ligands. Meanwhile, the structures, thermal analyses, luminescent properties, and magnetic properties were explored in detail.

**Received:** February 27, 2012
**Revised:** September 17, 2012
**Published:** October 11, 2012





dx.doi.org/10.1021/cg300277m | *Cryst. Growth Des.* 2012, 12, 5203–5210

**Table 1. Crystal Data and Structure Refinement for 1, 4, and 1a−5a**

| | 1 | 4 | 1a | 2a | 3a | 4a | 5a |
|---|---|---|---|---|---|---|---|
| formula | $C_{54}H_{46}Eu_4O_{35}$ | $C_{54}H_{46}Dy_4O_{35}$ | $C_{10}H_8EuO_8$ | $C_{10}H_8GdO_8$ | $C_{10}H_8TbO_8$ | $C_{10}H_8DyO_8$ | $C_{10}H_8HoO_8$ |
| fw | 1862.75 | 1904.91 | 408.12 | 413.41 | 415.08 | 418.66 | 421.09 |
| cryst syst | triclinic | triclinic | monoclinic | monoclinic | monoclinic | monoclinic | monoclinic |
| space group | $P\bar{1}$ | $P\bar{1}$ | $P21/c$ | $P21/c$ | $P21/c$ | $P21/c$ | $P21/c$ |
| $a$, Å | 7.745(3) | 7.7172(6) | 7.4137(3) | 7.3300(2) | 7.3327(6) | 7.3567(2) | 7.3194(6) |
| $b$, Å | 16.768(7) | 16.6793(13) | 7.1036(3) | 7.0421(2) | 7.0342(4) | 7.0497(2) | 7.0328(6) |
| $c$, Å | 21.273(9) | 21.1778(18) | 23.6243(11) | 23.4314(7) | 23.4468(11) | 23.4803(5) | 23.502(2) |
| $\alpha$, deg | 92.582(7) | 92.602(7) | 90 | 90 | 90 | 90 | 90 |
| ß, deg | 91.232(8) | 91.406(6) | 95.764(5) | 96.144(3) | 96.161(5) | 96.025(2) | 97.081(11) |
| $\gamma$, deg | 90.657(8) | 90.705(6) | 90 | 90 | 90 | 90 | 90 |
| $V$, Å$^3$ | 2759.1(19) | 2722.1(4) | 1237.86(9) | 1202.55(6) | 1202.39(13) | 1211.02(5) | 1200.59(18) |
| $Z$ | 2 | 2 | 4 | 4 | 4 | 4 | 4 |
| $D_c$, g/cm$^3$ | 2.242 | 2.324 | 2.190 | 2.283 | 2.293 | 2.296 | 2.330 |
| $F(000)$ | 1804 | 1828 | 780.0 | 784 | 788 | 792.0 | 796.0 |
| $\mu$, mm$^{-1}$ | 4.595 | 5.539 | 6.623 | 5.548 | 5.915 | 6.623 | 6.623 |
| GOF on $F^2$ | 1.043 | 0.985 | 1.123 | 1.062 | 1.079 | 1.026 | 1.093 |
| $R_1/wR_2(I > 2\sigma(I))$ | 0.0965/0.1579 | 0.0877/0.2242 | 0.0661/0.1817 | 0.0462/0.1193 | 0.0680/0.1605 | 0.0636/0.1603 | 0.0452/0.1011 |

**Scheme 1. Synthetic Strategy of 1−5 and 1a−5a**

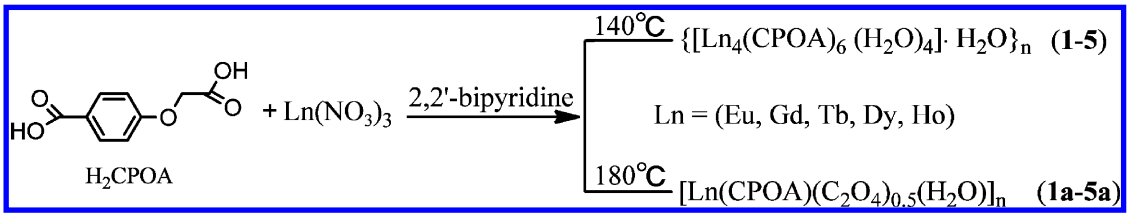


## EXPERIMENTAL SECTION

**Materials and General Characterization.** All of the chemicals were purchased and used without purification. Elemental analyses for C, H, and N were obtained at the Institute of Elemental Organic Chemistry, Nankai University. The FT-IR spectra were measured with a Bruker Tensor 27 spectrophotometer on KBr disks. TGA experiments were performed on a NETZSCH TG 209 instrument with a heating rate of 10 °C min$^{-1}$. Powder X-ray diffraction measurements were recorded on a D/Max-2500 X-ray diffractometer using Cu K$\alpha$ radiation. The magnetic properties were measured on a PPMS-9 ACMS magnetometer. Diamagnetic corrections were made with Pascal's constants for all the constituent atoms. The fluorescent spectra were measured on a F-4500 FL spectrophotometer.

**Synthesis.** *{[Ln$_4$(CPOA)$_6$(H$_2$O)$_4$]·H$_2$O}$_n$ (Ln = Eu (**1**), Gd (**2**), Tb (**3**), Dy (**4**), Ho (**5**))*. A mixture of $H_2$CPOA (0.0588 g, 0.3 mmol), 2,2′-bipyridine (0.032 g, 0.2 mmol), 0.2 mmol of Ln(NO$_3$)$_3$·6H$_2$O [Ln = Eu (0.0892 g); Gd (0.0902 g); Tb (0.0906 g); Dy (0.0913 g); Ho (0.0916 g)], and 8 mL of distilled water were sealed in a Teflon-lined stainless vessel (25 mL) and heated at 140 °C for 72 h under autogenous pressure. The vessel was then cooled slowly down to room temperature at 2 °C/h. Colorless strip crystals were obtained. The yield of **1**−**5** was 65, 42, 46, 39, and 31% (based on Ln(NO$_3$)$_3$·6H$_2$O), respectively. Elemental Anal. (%) Calcd for **1**: C, 34.82; H, 2.49. Found: C, 34.91; H, 2.65. Calcd for **2**: C, 34.43; H, 2.46. Found: C, 34.48; H, 2.63. Calcd for **3**: C, 34.30; H, 2.45. Found: C, 34.41; H, 2.52. Calcd for **4**: C, 34.05; H, 2.43. Found: C, 34.02; H, 2.38. Calcd for **5**: C, 33.87; H, 2.4. Found: C, 33.96; H, 2.35. IR (KBr, cm$^{-1}$): For **1**: 3420s, 1655s, 1521m, 1401s, 1262s. For **2**: 3415s, 1654s, 1520m, 1403s, 1262s. For **3**: 3420s, 1656s, 1521m, 1402s, 1262s. For **4**: 3430s, 1655s, 1524m, 1405s, 1262s. For **5**: 3425s, 1656s, 1520m, 1401s, 1263s.

*[Ln(CPOA)(C$_2$O$_4$)$_{0.5}$(H$_2$O)]$_n$ (Ln = Eu (**1a**), Gd (**2a**), Tb (**3a**), Dy (**4a**), Ho (**5a**))*. The synthetic methods of **1a**−**5a** were similar to those of **1**−**5** mentioned above, and the temperature was 180 °C instead of 140 °C. As a result, the colorless lamellar crystals of **1a**−**4a** and a reddish lamellar crystal of **5a** were obtained. The yield of **1a**−**5a** was 32, 23, 27, 29, and 21% (based on Ln(NO$_3$)$_3$·6H$_2$O), respectively. Elemental Anal. (%) Calcd for **1a**: C, 29.43; H, 1.98. Found: C, 29.20; H, 1.86. Calcd for **2a**: C, 29.05; H, 1.95. Found: C, 28.96; H, 1.87. Calcd for **3a**: C, 28.93; H, 1.94. Found: C, 28.74; H, 1.82. Calcd for **4a**: C, 28.69; H, 1.93. Found: C, 28.45; H, 1.79. Calcd for **5a**: C, 28.52; H, 1.91. Found: C, 28.37; H, 1.83. IR (KBr, cm$^{-1}$): For **1a**: 3465s, 1725m, 1660s, 1403s, 1332m, 1259s. For **2a**: 3436s, 1720m, 1661s, 1404s, 1333m, 1259s. For **3a**: 3442s, 1720m, 1661s, 1416s, 1333m, 1259s. For **4a**: 3450s, 1725m, 1665s, 1404s, 1334m, 1260s. For **5a**: 3462s, 1725m, 1667s, 1416s, 1334m, 1260s.

**Crystallography.** Crystallographic data of **1**, **4**, and **1a**−**5a** were collected on a SuperNova single crystal diffractometer equipped with graphite-monochromatic Mo K$\alpha$ radiation ($\lambda$ = 0.71073 Å). The data integration and empirical absorption corrections were carried out by SAINT programs. The structures were solved by direct methods (SHELXS 97). All the non-hydrogen atoms were refined anisotropically on $F^2$ by full-matrix least-squares techniques (SHELXL 97).[15] All hydrogen atoms except for those of the uncoordinated water molecules in these coordination polymers were generated geometrically and refined isotropically using the riding model.

Much effort has been made to obtain perfect crystals of **2**, **3**, and **5**, but failed. Therefore, details of the crystal parameters for only **1**, **4**, and **1a**−**5a** are summarized in Table 1.

## RESULTS AND DISCUSSION

**Syntheses.** To explore the temperature influence on the formation of the compounds, the experiments were conducted by simply changing the temperature from 140 to 180 °C without altering reagents. Compounds **1**−**5** were obtained at 140 °C, but during 150−170 °C, both **1**−**5** and **1a**−**5a** can be generated in one vessel. When the temperature went up to 180 °C, the compounds **1a**−**5a** were obtained alone (Scheme 1). The result implied that the reaction temperature may play a great role in separating or purifying crystal samples. Additionally, 2,2′-bipyridine also has a significant effect on the


dx.doi.org/10.1021/cg300277m | Cryst. Growth Des. 2012, 12, 5203−5210

crystallization of products, which may adjust the acid/base of the solution, although it does not embed the frameworks of structures.

**Description of the Crystal Structures.** *Crystal Structure of* $\{[Ln_4(CPOA)_6(H_2O)_4]\cdot H_2O\}_n$. Single-crystal X-ray diffraction analyses reveal that compounds **1** and **4** are isomorphous, crystallizing in the triclinic system with space group $P\bar{1}$, representatively; hence only the structure of compound **1** will be discussed in detail. Each asymmetric unit contains four independent $Eu^{3+}$ (Eu1, Eu2, Eu3, Eu4), six $CPOA^{2-}$ ligands, four coordinated water molecules, and one free water molecule. Both Eu1 and Eu2 are eight-coordinated with a distorted bicapped trigonal prism, which are all completed by one water molecule, five monodentate carboxylic oxygen atoms, and two bidentate-chelating oxygen atoms. Four monodentate-bridging carboxylic oxygen atoms, four bidentate-chelating carboxylic oxygen atoms, and one water molecule complete the nine-coordinated environment of Eu3 and Eu4 (Figure 1). The Eu–O distances are in the range of 2.307(16)–2.808(15) Å (Eu1–O), 2.303(17)–2.813(17) Å (Eu2–O), 2.27(3)–2.75(3) Å (Eu3–O), and 2.331(16)–2.76(2) Å (Eu4–O). The $CPOA^{2-}$ ligands exhibit three coordination modes: *A*, *B*, and *C* in Scheme 2, acting as a tetradentate metal linker. The ligands connect Eu1 and Eu2 into a 2D plane, which was further linked by one 1D chain constituted by Eu3 and Eu4 into an interesting 3D framework (Figure 2).

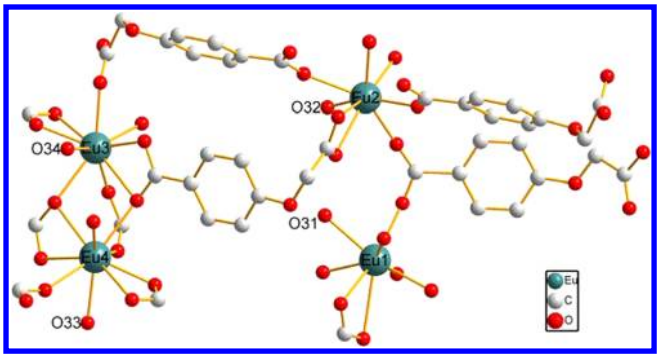


**Figure 1.** Coordinated environment of $Eu^{3+}$ in compound **1**.

*Crystal Structure of* $[Ln(CPOA)(C_2O_4)_{0.5}(H_2O)]_n$. Single-crystal X-ray diffraction analyses reveal that compounds **1a–5a** are isomorphous, belonging to the monoclinic system with space group $P21/c$, representatively; hence only the structure of compound **4a** will be discussed in detail. Each asymmetric unit contains one unique $Dy^{3+}$, one $CPOA^{2-}$ ligand, one water molecule, and half an oxalate anion. The eight-coordinated $Dy^{3+}$, which is completed by five carboxylic oxygen atoms of four $CPOA^{2-}$ liands, one oxygen atom of one water molecule, and two oxygen atoms of one oxalate anion, can be described as a distorted bicapped trigonal prism in which O1 and O5 act as the capping atoms (Figure 3, left). The Dy–O distances are in the range of 2.267(10)–2.585(10) Å. The $CPOA^{2-}$ ligands adopt only one coordination mode *A* in Scheme 2, acting as a tetradentate metal linker. The $Dy^{3+}$ is bridged by the oxalate and the $\mu_2$-O into a 1D chain along the *a* direction. The chains are connected by the carboxylic oxygen atoms of $CPOA^{2-}$ ligands into a 2D plane (Figure 3, middle), which is further linked by the $CPOA^{2-}$ ligands into a 3D framework. The binuclear Dy units linked by carboxylic oxygen atoms (O2) and the $CPOA^{2-}$ ligands can be considered as 8-connected and 3-connected nodes, respectively, and the oxalate anions are simplified as lines. The structure can be simplified as a 3,8-connected framework with the point (Schlafli) symbol $\{4.5^2\}_2\{4^2.5^6.6^{14}.7^2.8^4\}$, as shown in Figure 3.

Zhang,[16a] Hong,[16c] and their co-workers considered that the oxalate anions may be generated via an in situ oxidation–hydrolysis reaction of the organic acid in high temperature, and spontaneously, the metal ions may act as catalysis for the decomposition of the organic acid.[16b] Therefore, the oxalate anions in **1a–5a** may be originated from the decomposition of $H_2CPOA$ molecules under high temperature and the catalysis of lanthanide ions.

Three 1D compounds, La, Pr, Nd, and one 3D compound, La, were obtained at 120 °C in our previous work[14] based on this ligand. UV and magnetic properties were detected and analyzed. Compounds **1–5** and **1a–5a** were synthesized at higher reaction temperatures than that in the previous work.[14] The structural dimensionalities of these compounds change from 1D chains[14] to 3D frameworks in this work. Thus, we found that the temperature played a key role in constructing coordination polymers. Compared with the analogous rigid ligand terephthalic acid,[1d] $H_2CPOA$ has one flexible $-OCH_2$ spacer, which easily tunes structures by changing coordination modes of $H_2CPOA$.

**IR Spectra, Powder X-ray Diffraction, and Thermogravimetric Analysis (TGA).** For the $H_2CPOA$ ligand, the characteristic absorption bands at ~1260 $cm^{-1}$ occurred in the IR spectrum, which is attributable to the C–O–C stretching vibrations of the $C_{Ph}$–O–$CH_2$ groups (Ph = benzene). The strong bands at 1360–1650 $cm^{-1}$ for all compounds are characteristic of the carboxyl groups. The broad absorption bands in the range of 3500–3410 $cm^{-1}$ indicate the presence of water molecules in the structures. The ~1720 $cm^{-1}$ in compounds **1a–5a** is characteristic of the oxalate group.

The PXRD patterns for **1–5** are in conformity with the simulated one from the single-crystal data of **1**, demonstrating that compounds **1–5** are isomorphic and proving the purity of samples **1–5**. The PXRD patterns of **1a–5a** have been also examined, and they are well consistent with the simulated one of **4a**, indicating that they are isomorphic and proving the purity of the samples (Figure 4).

**Scheme 2. Coordination Modes of $CPOA^{2-}$**

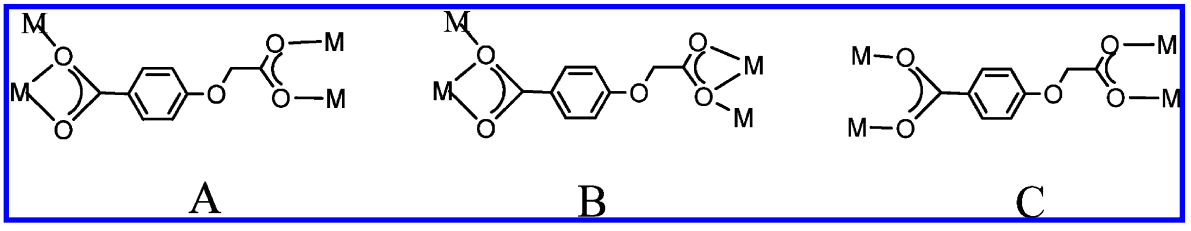



dx.doi.org/10.1021/cg300277m | Cryst. Growth Des. 2012, 12, 5203–5210

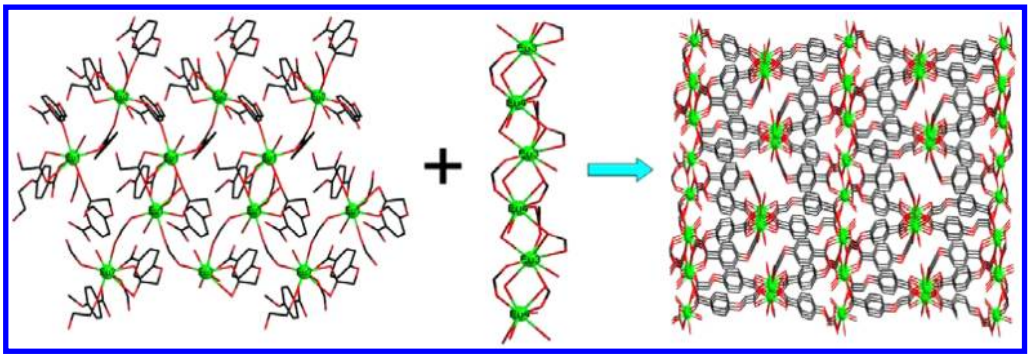

**Figure 2.** In compound **1**, 2D plane consisted of Eu1 and Eu2 (left), 1D chain constituted by Eu3 and Eu4 (middle), and 3D framework (right). Color codes: red, O; black, C; green, Eu.

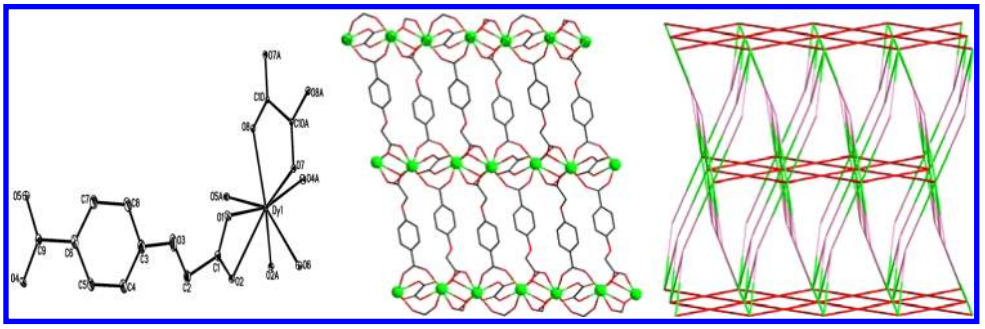

**Figure 3.** Coordinated environment of $Dy^{3+}$ in compound **4a** (left). The 2D plane of compound **4a** (color codes: red, O; black, C; green, Dy) (middle). The topology of compound **4a**; the green acts as the $Dy_2O_2$ unit, the pink acts as the $CPOA^{2-}$ ligands, and the red lines act as oxalate linkers (right).

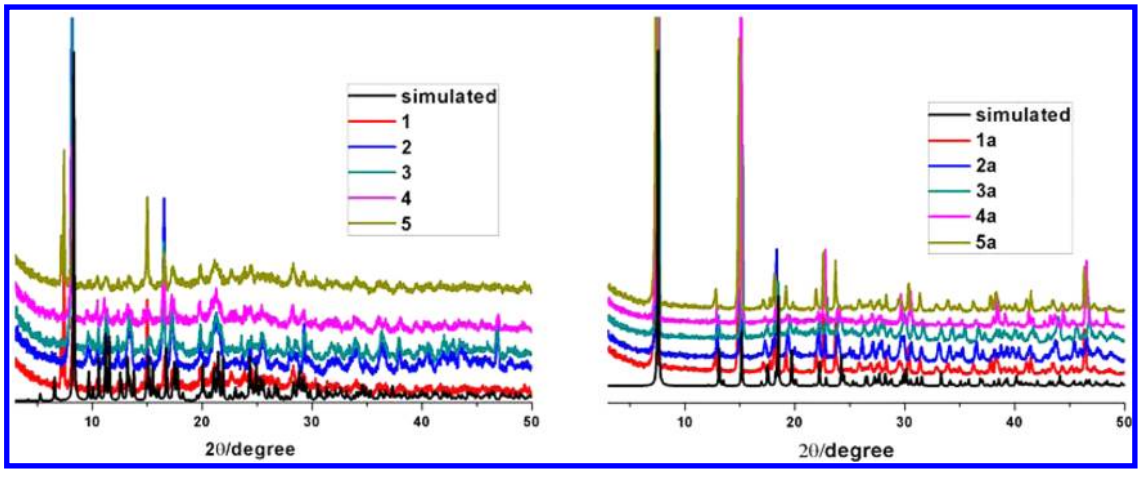


**Figure 4.** PXRD patterns of compounds **1**−**5** and the simulated one of **1** (left), and the PXRD patterns of compounds **1a**−**5a** and the simulated one of **4a** (right).

To study the thermal stability of the compounds and further affirm the molecular formula of the compounds **2**−**5** and **2a**−**3a**, compounds **1**−**5** and **1a**−**3a** were detected in the range of 25−800 °C. The TGA curves of **1**−**5** exhibit two regions of weight loss. The first weight loss of **1**−**5** between 100 and 260 °C is 4.54, 4.51, 4.47, 4.38, and 4.36%, respectively, and they correspond to the loss of four coordinated water molecules and one free water molecule, being identical with the calculated 4.83% for **1**, 4.78% for **2**, 4.76% for **3**, 4.72% for **4**, and 4.70% for **5**. The second weight loss above 430 °C stems from the decomposition of the 3D frameworks in **1**−**5**. Additionally, thermal analysis of the $H_2$CPOA ligand was also conducted (Figure S3, Supporting Information), and the ligand begins to decompose at 270 °C. However, in preparing compounds **1a**−**5a**, the decomposition of part $H_2$CPOA ligand at 180 °C may benefit from the higher pressure in the Teflon-lined stainless vessel under hydrothermal condition. On the basis of the analyses mentioned above, we can conclude that, during 260−430 °C, the 3D frameworks of **1**−**5** still remain intact after removing coordinated water molecules, and the corresponding formula of these compounds may be written as $[Ln_4(CPOA)_6]_n$. For **1a**−**3a**, the first weight loss of 4.58% for **1a**, 4.20% for **2a**, and 4.12% for **3a** between 290 and 370 °C corresponds to the loss of one coordinated water molecule, which is well consistent with the calculated values (**1a**: 4.41%; **2a**: 4.35%; **3a**: 4.33%). Upon increasing the temperature, the frameworks of **1a**−**3a** commence to collapse (Figure 5).


dx.doi.org/10.1021/cg300277m | *Cryst. Growth Des.* 2012, 12, 5203−5210

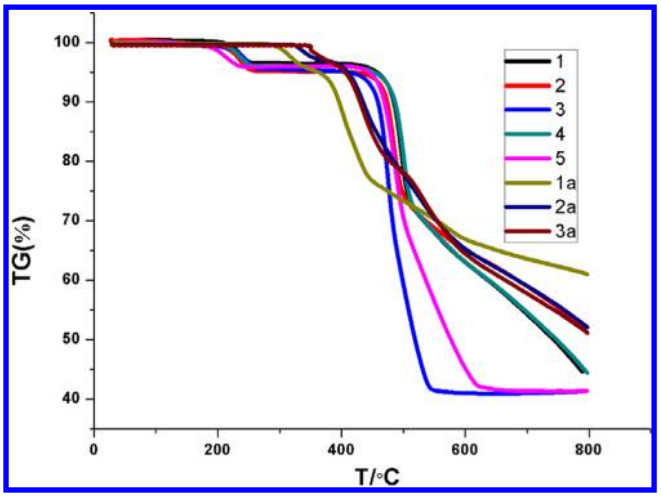


**Figure 5.** TGA curves of compounds **1**−**5** and **1a**−**3a**.

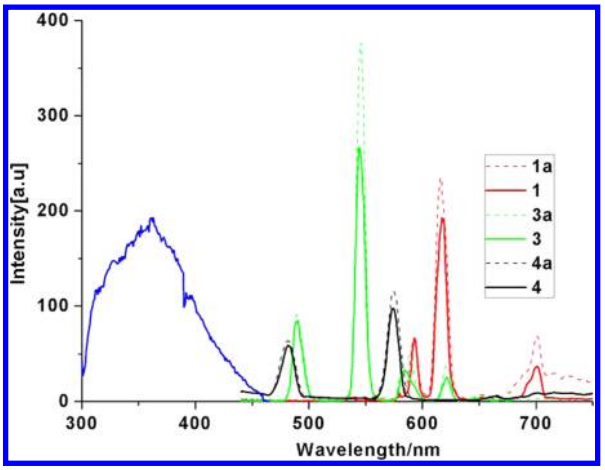


**Figure 6.** Solid-state emission spectra of $H_2$CPOA ($\lambda_{ex}$ = 290 nm) (blue), **1** and **1a** ($\lambda_{ex}$ = 290 nm) (red), **3** and **3a** ($\lambda_{ex}$ = 292 nm) (green), and **4** and **4a** ($\lambda_{ex}$ = 290 nm) (black).

**Luminescent Properties.** Considering the excellent luminescent properties of $Eu^{3+}$, $Tb^{3+}$, and $Dy^{3+}$, the solid-state photoluminescent spectra of **1**, **1a**, **3**, **3a**, **4**, and **4a** were measured at room temperature. The solid $H_2$CPOA ligand shows an emission band at 363 nm upon the excitation at 290 nm, which may be assigned to the $\pi^* \rightarrow$ n electron transition. Intense red luminescence and typical emission bands of $Eu^{3+}$ emerge in the emission spectra of compounds **1** and **1a** upon excitation at 290 nm.[17] The weaker band at 536 nm for **1** and 537 nm for **1a** originated from the $^5D_1 \rightarrow {}^7F_1$ transition. The stronger emission spectra are assigned to the $^5D_0 \rightarrow {}^7F_J$ ($J$ = 0, 1, 2, 3, 4) transitions. As is known, the transition of $^5D_0 \rightarrow {}^7F_0$ is only allowable for $C_s$, $C_n$, and $C_{nv}$ ($n$ = 1, 2, 3, 4, 5, 6) site symmetries.[18] According to that described above, **1** and **1a** crystallize in the triclinic and monoclinic crystal systems, and the $Eu^{3+}$ belongs to the symmetry of $C_1$ and $C_2$, respectively. Thus, the $^5D_0 \rightarrow {}^7F_0$ transitions observed in the emission spectra of **1** and **2** (580 nm) are not unreasonable. The most intensive bands at 617 nm for **1** and 615 nm for **1a** are assigned to the $^5D_0 \rightarrow {}^7F_2$ electric dipole transition, which dominates the red light emission. The bands at 594 nm for **1** and 593 nm for **1a** may be assigned to the $^5D_0 \rightarrow {}^7F_1$ magnetic dipole transition. Additionally, the intensity of the $^5D_0 \rightarrow {}^7F_2$ transition in **1** is 3.5 times stronger than that of the $^5D_0 \rightarrow {}^7F_1$ transition, supporting the low symmetry of the Eu center.[19] The bands at 701 nm for **1** and 700 nm for **1a** are weaker, assigned to the $^5D_0 \rightarrow {}^7F_4$ transitions. The bands at 651 nm for **1** and 652 nm for **1a** are assigned to the $^5D_0 \rightarrow {}^7F_3$ transitions (Figure 6).

The emission spectra of compounds **3** and **3a** exhibit characteristic bands of $Tb^{3+}$ and a strong green luminescence upon excitation at 292 nm, designated as the $^5D_4 \rightarrow {}^7F_J$ ($J$ = 6, 5, 4, 3) transitions.[20] The strongest emission peaks at 544 nm for **3** and 545 nm for **3a** are assigned to the $^5D_4 \rightarrow {}^7F_5$ transitions. The emission peaks at 488 nm for **3** and 489 nm for **3a** are assigned to the $^5D_4 \rightarrow {}^7F_6$ transitions. The peaks at 583 nm for **3** and 585 nm for **3a** are assigned to the $^5D_4 \rightarrow {}^7F_4$ transitions, and the weakest emission peaks at 621 nm for **3** and 622 nm for **3a** are assigned to the $^5D_4 \rightarrow {}^7F_3$ transitions.

The spectra of compounds **4** and **4a** display the typical bands of $Dy^{3+}$ and an intense yellow luminescence upon excitation at 290 nm with two main bands at 481, 575 nm and 482, 574 nm, respectively, ascribed to the $^4F_{5/2} \rightarrow {}^6H_{13/2}$ and $^4F_{5/2} \rightarrow {}^6H_{15/2}$ transitions. After that, the weaker bands at 663 nm for **4** and 662 nm for **4a** are assigned to the $^4F_{5/2} \rightarrow {}^6H_{11/2}$ transitions (Figure 6).[21]

Obviously, the emission intensity of compounds **1a**, **3a**, and **4a** is stronger than that of compounds **1**, **3**, and **4**, respectively. The phenomenon may be explained by the different coordination environments of $Ln^{3+}$. Both eight- and nine-coordinated $Ln^{3+}$ coexist in **1**−**5**, whereas only eight-coordinated $Ln^{3+}$ is in **1a**−**5a**. They possess the same coordinated water molecules, but it should be noted that, in **1a**−**5a**, the existence of the bridging $C_2O_4^{2-}$ may transfer effectively energy to lanthanide centers, enhancing the emission intensity. In consideration of the strong luminescence of Tb and Eu compounds, **1**, **1a**, **3**, and **3a** may serve as luminescent materials.

**Magnetic Properties.** Investigating the magnetic properties of lanthanide compounds has been a complicated and difficult problem as a result of the unquenched first-order orbital momentum of lanthanide ions (except for $Gd^{3+}$) under the ligand-field effect.[22,23] As is known, the $4f^n$ configuration of $Ln^{3+}$ is split into $^{2S+1}L_J$ states by the interelectronic repulsion and spin−orbit coupling, and can be further split into Stark components ($2J$ + 1 if $n$ is even, $J$ + 1/2 if $n$ is odd; $n$: the number of electrons) under the crystal-field perturbation. With cooling the temperature, the depopulation of the Stark sublevels will lead to a decline in the value of $\chi_M T$, which may shield the weak ferromagnetic/antiferromagnetic coupling nature between adjacent lanthanide ions. Therefore, one cannot determine the magnetic interaction accurately based simply on the trend of $\chi_M T$.

Variable-temperature magnetic susceptibility measurements were carried out for samples **2**−**4** and **2a**−**4a** in the range of 2−300 K at an applied field of 1000 Oe, and the $\chi_M T$ versus $T$ plots are shown in Figure 7. For compounds **2**, **3**, and **4**, the value of $\chi_M T$ is 31.45, 47.15, and 56.29 $cm^3$ K $mol^{-1}$ at room temperature, respectively, which is close to the theoretical value of 31.52, 47.52, and 56.68 $cm^3$ K $mol^{-1}$ for the unit of four paramagnetic $Ln^{3+}$ ($Gd^{3+}$, $^8S_{7/2}$, $g$ = 2; $Tb^{3+}$, $^7F_6$, $g$ = 3/2; $Dy^{3+}$, $^6H_{15/2}$, $g$ = 4/3). With lowering the temperature, the $\chi_M T$ value of **2**−**4** decreases gradually and reaches the minimum value of 29.97, 21.95, and 30.86 $cm^3$ K $mol^{-1}$ at 2 K, respectively. $1/\chi_M$ versus $T$ further elucidates such behaviors (Figure S1, Supporting Information). The analysis of the magnetic data through the Curie−Weiss law in the equation, $\chi_M = C/(T - \theta)$,


dx.doi.org/10.1021/cg300277m | Cryst. Growth Des. 2012, 12, 5203−5210

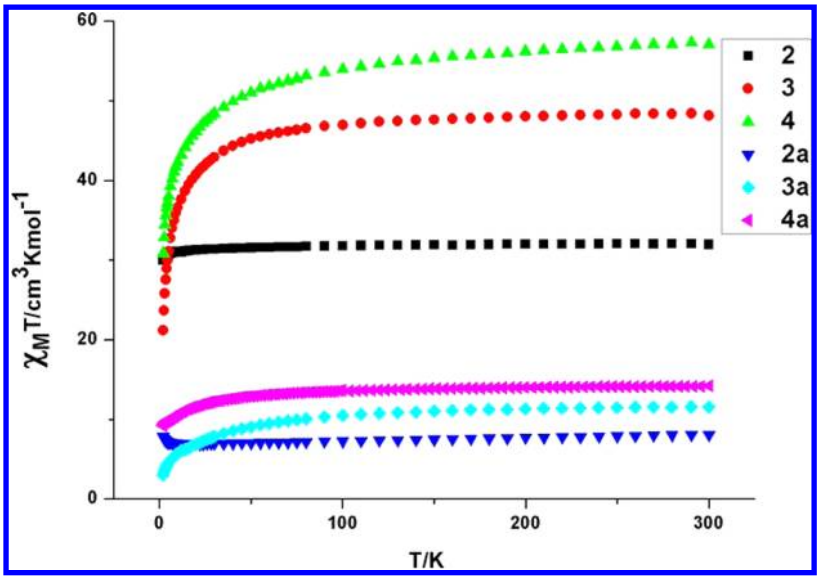


**Figure 7.** The plots of $\chi_M T$ vs T for **2**, **3**, **4**, **2a**, **3a**, and **4a**.

led to $C$ = 32.05 cm$^3$ K mol$^{-1}$, $\theta$ = −0.54 K for **2**; $C$ = 48.88 cm$^3$ K mol$^{-1}$, $\theta$ = −3.62 K for **3**; and $C$ = 57.65 cm$^3$ K mol$^{-1}$, $\theta$ = −4.76 K for **4**. For **2**, such behavior indicates the antiferromagnetic coupling between adjacent $Gd^{3+}$.[23] For **3** and **4**, such a phenomenon cannot imply the existence of the antiferromagnetic interactions between adjacent $Tb^{3+}/Dy^{3+}$ because of the strong spin−orbit coupling of $Tb^{3+}/Dy^{3+}$ coming from the strong unquenched orbital angular momentum.

For compounds **2a**, **3a**, and **4a**, the $\chi_M T$ value at room temperature is 7.79, 11.54, and 14.15 cm$^3$ K mol$^{-1}$, respectively, which is close to the theoretical value of 7.88, 11.82, 14.17 cm$^3$ K mol$^{-1}$ based on one $Ln^{3+}$ ($Gd^{3+}$, $^8S_{7/2}$, $g$ = 2; $Tb^{3+}$, $^7F_6$, $g$ = 3/2; $Dy^{3+}$, $^6H_{15/2}$, $g$ = 4/3). Upon lowering the temperature, the $\chi_M T$ value of compound **2a** decreases to 6.91 cm$^3$ K mol$^{-1}$ at 15 K, indicative of weak antiferromagnetic interaction between adjacent $Gd^{3+}$.[24] On further cooling, the sudden enhancement up to 7.81 cm$^3$ K mol$^{-1}$ at 2 K was observed, which may be originated from the weak ferromagnetic coupling between adjacent chains consisting of $Gd^{3+}$. Such a case has occurred in some Gd-based complexes.[25] For compounds **3a** and **4a**, the $\chi_M T$ value decreases slowly with cooling the temperature from 300 to 50 K and more rapidly below 50 K, reaching the minimum values of 2.98 and 9.18 cm$^3$ K mol$^{-1}$ at 2 K, respectively. On account of the large spin−orbit coupling of $Tb^{3+}/Dy^{3+}$, such behavior cannot be exactly ascribed to the antiferromagnetic coupling between adjacent $Tb^{3+}/Dy^{3+}$. $1/\chi_M$ versus $T$ obeys the Curie−Weiss law in the equation, $\chi_M = C/(T - \theta)$, with $C$ = 7.95 cm$^3$ K mol$^{-1}$, $\theta$ = −4.18 K for **2a**; $C$ = 11.95 cm$^3$ K mol$^{-1}$, $\theta$ = −11.33 K for **3a**; and $C$ = 14.31 cm$^3$ K mol$^{-1}$, $\theta$ = −4.55 K for **4a**.

To explore the dynamics of the magnetization, the alternating current (ac) susceptibility measurements of **4** and **4a** were carried out under a zero direct current (dc) magnetic field in the frequency range of 111−2311 Hz. As shown in Figure 8, the out-of-phase signal ($\chi_M''$) of **4** shows the strong frequency dependence, demonstrating the existence of magnetic relaxation behavior. The case was similar to the reported 2D $[Dy\text{-}(citrate)(H_2O)]_n$,[10a] and 3D $[Dy_2Co_2(2,5\text{-}pydc)_6(H_2O)_4]_n{\cdot}2nH_2O$.[10b] Unfortunately, the peaks were not observed as the result of the fast quantum tunneling. Thus, the

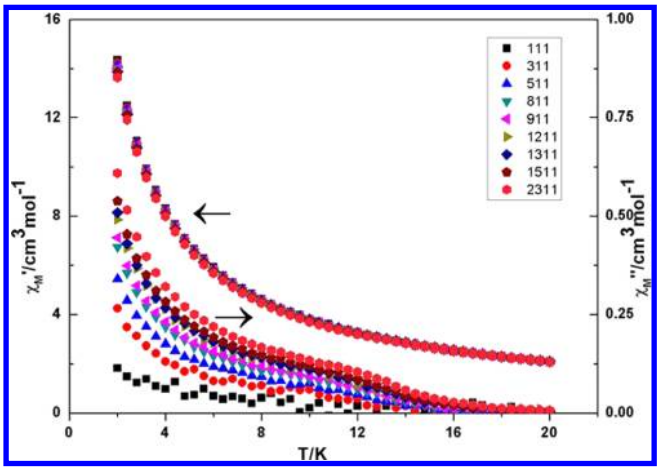


**Figure 8.** Temperature dependence of the in-phase ($\chi_M'$) and out-of-phase ($\chi_M''$) signals of the ac susceptibility for compound **4**.

energy barrier and relaxation time cannot be obtained by fitting the Arrhenius equation. On the basis of the assumption that a single relaxation process exists in compound **4**, the energy barrier and relaxation time can be roughly estimated from fitting the *ac* susceptibility by adopting the Debye model and equation, $\ln(\chi''/\chi') = \ln(\omega\tau_0) + E_a/k_BT$, yielding the energy barrier $E_a/k_B \approx 0.55$ K and the relaxation time $\tau_0 \approx 4 \times 10^{-6}$ s (Figure 9). This method has been applied in many compounds, but the values of the energy barrier and relaxation time are not accurate enough.[26] The $\chi_M''$ of **4a** is very weak, hardly showing a frequency dependence (Figure S2, Supporting Information).

It is well-known that the effect of the ligand field plays a significant role in the splitting of the ground-state multiplet of $Dy^{3+}$, resulting in interesting magnetic behaviors of Dy-based compounds, such as mononuclear Dy-SMM[9a] and two step relaxation behaviors.[2a] The giant magnetic difference between **4** and **4a** should originate from their different coordination environments of $Dy^{3+}$. Generally, the carboxyl groups bridging adjacent lanthanide ions transfer weak magnetic interaction due to the unique inner-layer 4f electrons, and therefore, the slow magnetic relaxation in **4** may result from the single-ion behavior of $Dy^{3+}$.[9a] Moreover, compound **2a** displays the ferromagnetic


dx.doi.org/10.1021/cg300277m | *Cryst. Growth Des.* 2012, 12, 5203−5210

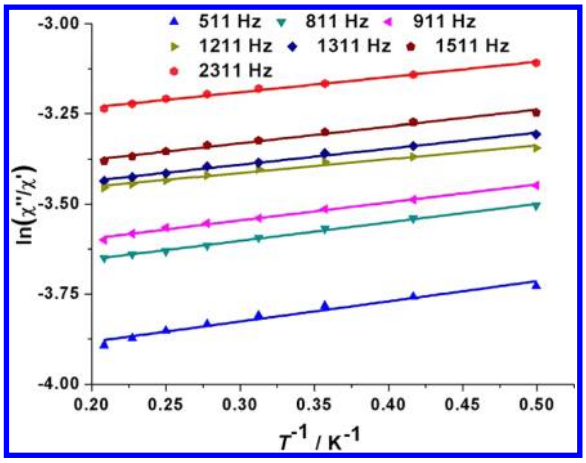


**Figure 9.** Plots of natural logarithm of $\chi''/\chi'$ vs $T^{-1}$ for **4**; the solid line represents the fitting in the range of 2.0−4.8 K.

interaction at low temperature, whereas compound **2** exhibits the antiferromagnetic interaction. This case may originate from the oxalate anions in **2a**, which may modulate the magnetic interaction between adjacent $Gd^{3+}$.

## CONCLUSIONS

Two series of 3D lanthanide−organic frameworks have been prepared by a hydrothermal method simply under different temperatures. The ligand decomposed partly with increasing the temperature and resulted in two types of frameworks. Solid luminescence of compounds **1** and **1a**, **3** and **3a**, and **4** and **4a** display the characteristic bands of $Eu^{3+}$, $Tb^{3+}$, and $Dy^{3+}$, respectively. Magnetic properties of **2**−**4** and **2a**−**4a** were investigated, and the alternating current (ac) susceptibility of **4** exhibits the strong frequency dependence, indicative of the existence of magnetic relaxation behavior. To our knowledge, such an interesting magnetic phenomenon is relatively rare in reported lanthanide-based MOFs.[10]

## ASSOCIATED CONTENT

### Supporting Information

X-ray crystallographic files in CIF format, TG curve of the $H_2$CPOA ligand, $1/\chi_M$ vs $T$, and ac susceptibility measurements of **4a**. This material is available free of charge via the Internet at http://pubs.acs.org.

## AUTHOR INFORMATION

### Corresponding Author

*E-mail: zhaobin@nankai.edu.cn (B.Z.). Fax: +86-22-23502458.

### Notes

The authors declare no competing financial interest.

## ACKNOWLEDGMENTS

This work was supported by NSFC (20971074, 91122004), FANEDD (200732), the NSF of Tianjin (10JCZDJC21700), and the 973 Program (2011CB935902 and 2012CB821702).

## REFERENCES

(1) (a) Rocha, J.; Carlos, L. D.; Almeida Paza, F. A.; Ananias, D. *Chem. Soc. Rev.* **2011**, *40*, 926. (b) Furukawa, H.; Ko, N.; Go, Y. B.; Aratani, N.; Choi, S. M.; Choi, E.; ÖzgürYazaydin, A.; Snurr, R. Q.; O'Keeffe, M.; Kim, J.; Yaghi, O. M. *Science* **2010**, *329*, 424. (c) Férey, G. *Chem. Soc. Rev.* **2008**, *37*, 191. (d) Li, H. L.; Eddaoudi, M.; O'Keeffe, M.; Yaghi, O. M. *Nature* **1999**, *402*, 276.

(2) (a) Guo, Y. N.; Xu, G. F.; Gamez, P.; Zhao, L.; Lin, S. Y.; Deng, R. P.; Tang, J. K.; Zhang, H. J. *J. Am. Chem. Soc.* **2010**, *132*, 8538. (b) Kurmoo, M. *Chem. Soc. Rev.* **2009**, *38*, 1353. (c) Gamer, M. T.; Lan, Y. H.; Roesky, P. W.; Powell, A. K.; Clérac, R. *Inorg. Chem.* **2008**, *47*, 6581.

(3) (a) Carlos, L. D.; Ferreira, R. A. S.; Bermudez, V. Z.; Julián-López, B.; Escribano, P. *Chem. Soc. Rev.* **2011**, *40*, 536. (b) Zhang, Z.-H.; Song, Y.; Okamura, T.-a.; Hasegawa, Y.; Sun, W.-Y.; Ueyama, N. *Inorg. Chem.* **2006**, *45*, 2896.

(4) (a) Wei, W.; Lu, Y.; Chen, W.; Chen, S. *J. Am. Chem. Soc.* **2011**, *133*, 2060. (b) Lian, P.; Wei, H. B.; Zheng, C.; Nie, Y. F.; Bian, J.; Bian, Z. Q.; Huang, C. H. *Dalton Trans.* **2011**, *40*, 5476. (c) Pellegatti, L.; Zhang, J.; Drahos, B.; Villette, S.; Suzenet, F.; Guillaumet, G.; Petoud, S.; Tóth, E. *Chem. Commun.* **2008**, 6591.

(5) (a) Sivakumar, S.; Reddy, M. L. P.; Cowley, A. H.; Butorac, R. R. *Inorg. Chem.* **2011**, *50*, 4882. (b) Kobayashi, Y.; Jacobs, B.; Allendorf, M. D.; Long, J. R. *Chem. Mater.* **2010**, *22*, 4120.

(6) (a) Shi, F. N.; Cunha-Silva, L.; SáFerreira, R. A.; Mafra, L.; Trindade, T.; Carlos, L. D.; Paz, F. A. A.; Rocha, J. *J. Am. Chem. Soc.* **2008**, *130*, 150. (b) Chandler, B. D.; Cramb, D. T.; Shimizu, G. K. H. *J. Am. Chem. Soc.* **2006**, *128*, 10403.

(7) (a) Amghouz, Z.; Roces, L.; García-Granda, S; Garcia, J. R.; Souhail, B.; Mafra, L.; Shi, F. N.; Rocha. *J. Inorg. Chem.* **2010**, *49*, 7917. (b) Vitorino, M. J.; Devic, T.; Tromp, M.; Férey, G.; Visseaux, M. *Chem. Phys.* **2009**, *210*, 1923. (c) Cunha-Silva, L.; Lima, S.; Ananias, D.; Silva, P.; Mafra, L.; Carlos, L. D.; Pillinger, M.; Valente, A. A.; Paz, F. A. A.; Rocha, J. *J. Mater. Chem.* **2009**, *19*, 2618.

(8) (a) Layfield, R. A.; McDouall, J. J. W.; Sulway, S. A.; Tuna, F.; Collison, D.; Winpenny, R. E. P. *Chem.—Eur. J.* **2010**, *16*, 4442. (b) Zheng, Y. Z.; Lan, Y. H.; Wernsdorfer, W.; Anson, C. E.; Powell, A. K. *Chem.—Eur. J.* **2009**, *15*, 12566. (c) Wang, B. W.; Jiang, S. D.; Wang, X. T.; Gao, S. *Sci. China, Ser. B: Chem.* **2009**, *52*, 1739. (d) Ishikawa, N.; Sugita, M.; Tanaka, N.; Ishikawa, T.; Koshihara, S. Y.; Kaizu, Y. *Inorg. Chem.* **2004**, *43*, 18.

(9) (a) Jiang, S. D.; Wang, B. W.; Su, G.; Wang, Z. M.; Gao, S. *Angew. Chem., Int. Ed.* **2010**, *49*, 7448. (b) Lin, P. H.; Burchell, T. J.; Clerac, R.; Murugesu, M. *Angew. Chem., Int. Ed.* **2008**, *47*, 8848. (c) Tang, J. K.; Hewitt, I.; Madhu, N. T.; Chastanet, G.; Wernsdorfer, W.; Anson, C. E.; Benelli, C.; Sessoli, R.; Powell, A. K. *Angew. Chem., Int. Ed.* **2006**, *45*, 1729.

(10) (a) Li, F. Y.; Xu, L.; Gao, G. G.; Fan, L. H.; Bi, B. *Eur. J. Inorg. Chem.* **2007**, 3405. (b) Huang, Y. G.; Wang, X. T.; Jiang, F. L.; Gao, S.; Wu, M. Y.; Gao, Q.; Wei, W.; Hong, M. C. *Chem.—Eur. J.* **2008**, *14*, 10340. (c) Chen, Z.; Zhao, B.; Cheng, P.; Zhao, X. Q.; Shi, W.; Song, Y. *Inorg. Chem.* **2009**, *48*, 3493.

(11) (a) Chen, B.; Xiang, S.; Qiang, G. *Acc. Chem. Res.* **2010**, *43*, 1115. (b) Chen, B. L.; Wang, L. B.; Xiao, Y. Q.; Fronczek, F. R.; Xue, M.; Cui, Y. J.; Qian, G. D. *Angew. Chem., Int. Ed.* **2009**, *48*, 500. (c) Zhao, B.; Chen, X. Y.; Cheng, P.; Liao, D. Z.; Yan, S. P.; Jiang, Z. H. *J. Am. Chem. Soc.* **2004**, *126*, 15394.

(12) (a) Herm, Z. R.; Swisher, J. A.; Smit, B.; Krishnai, R.; Long, J. R. *J. Am. Chem. Soc.* **2011**, *133*, 5664. (b) Zhao, B.; Cheng, P.; Chen, X. Y.; Cheng, C.; Shi, W.; Liao, D. Z.; Yan, S. P.; Jiang, Z. H. *J. Am. Chem. Soc.* **2004**, *126*, 3012. (c) Eddaoudi, M.; Kim, J.; Rosi, N.; Vodak, D.; Wachter, J.; O'Keeffe, M.; Yaghi, O. M. *Science* **2002**, *295*, 5554.

(13) (a) Aijaz, A.; Lama, P.; Bharadwaj, P. K. *Eur. J. Inorg. Chem.* **2010**, *24*, 3829. (b) Zhuang, W. J.; Zheng, X. J.; Li, L. C.; Liao, D. Z.; Ma, H.; Jin, L. P. *CrystEngComm* **2007**, *9*, 653. (c) Cheng, X. N.; Zhang, W. X.; Zheng, Y. Z.; Chen, X. M. *Chem. Commun.* **2006**, 3603. (d) Zhang, X. F.; Gao, S.; Huo, L. H.; Zhao, J. G. *Acta Crystallogr., Sect. E* **2005**, *61*, 2471. (e) Deng, Z. P.; Gao, S.; Huo, L. H.; Zhao, H. *Acta Crystallogr., Sect. C* **2005**, *61*, 523. (f) Wai, H. Y.; Ru, J. W.; Mark, T. C. W. *J. Crystallogr. Spectrosc. Res.* **1990**, *20*, 307. (g) Kennard, C. H. L.; Smith, G.; O'Reilly, E. J. *Inorg. Chim. Acta* **1984**, *82*, 35.

(14) Chen, Z.; Cui, P.; Zhang, Y.; Zhao, B. *Chin. Sci. Bull.* **2009**, *54*, 4296.

(15) (a) Sheldrick, G. M. *SHELXS-97: Program for the Solution of Crystal Structures*; University of Göttingen: Göttingen, Germany, 1997. (b) Sheldrick, G. M. *SHELXL-97: Program for the Refinement of Crystal Structures*; University of Göttingen: Göttingen, Germany, 1997.
(16) (a) Zhang, X. M. *Coord. Chem. Rev.* **2005**, *249*, 1201. (b) Zhang, X. M.; Wu, H. S.; Chen, X. M. *Eur. J. Inorg. Chem.* **2003**, *42*, 2959. (c) Li, X.; Cao, R.; Sun, D.; Shi, Q.; Bi, W.; Hong, M. *Inorg. Chem. Commun.* **2003**, *6*, 815.
(17) Vicentini, G.; Zinner, L. B.; Zukerman-Schpector, J.; Zinner, K. *Coord. Chem. Rev.* **2000**, *196*, 353.
(18) (a) Chen, X. Y.; Liu, G. K. J. *Solid State Chem.* **2005**, *178*, 419. (b) Xu, Q. H.; Li, L. S.; Liu, X. S.; Xu, R. R. *Chem. Mater.* **2002**, *14*, 549.
(19) Kirby, A. F.; Foster, D.; Richardson, F. S. *Chem. Phys. Lett.* **1983**, *95*, 507.
(20) Tedeschi, C.; Azema, J.; Gornitzka, H.; Tisnes, P.; Picard, C. *Dalton Trans.* **2003**, 1738.
(21) Arnaud, N.; Vaquer, E.; Georges, J. *Analyst* **1998**, *123*, 261.
(22) Kahn, M. L.; Ballou, R.; Porcher, P.; Kahn, O.; Sutter, J. P. *Chem.—Eur. J.* **2002**, *8*, 525.
(23) (a) Costes, J. P.; Dahan, F.; Dupuis, A. *Inorg. Chem.* **1998**, *37*, 153. (b) Liu, S.; Gelmini, L.; Rettig, S. J. *J. Am. Chem. Soc.* **1992**, *114*, 6081.
(24) (a) Zhang, A. J.; Wang, Y. W.; Dou, W.; Dong, M.; Zhang, Y. L.; Tang, Y.; Liu, W. S.; Peng, Y. *Dalton Trans.* **2011**, *40*, 2844. (b) Costes, J. P.; Clemente-Juan, J. M.; Dahan, F. *Angew. Chem., Int. Ed.* **2002**, *41*, 323.
(25) (a) Hatscher, S. T.; Urland, W. *Angew. Chem., Int. Ed.* **2003**, *42*, 2862. (b) Molina, M. H.; Pérez, C. R.; López, T.; Lloret, F.; Julve, M. *Inorg. Chem.* **2003**, *42*, 5457.
(26) (a) Bartolomé, J.; Filoti, G.; Kuncser, V.; Schinteie, G.; Mereacre, V.; Anson, C. E.; Powell, A. K.; Prodius, D.; Turta, C. *Phys. Rev. B* **2009**, *80*, 014430. (b) Lin, S.-Y.; Xu, G.-F.; Zhao, L.; Guo, Y.-N.; Guo, Y.; Tang, J.-K. *Dalton Trans.* **2011**, *40*, 8213.